

Four-Electron Oxidation of Phenols to *p*-Benzoquinone Imines by a (Salen)ruthenium(VI) Nitrido Complex

Jianhui Xie,[†] Wai-Lun Man,[†] Chun-Yuen Wong,[†] Xiaoyong Chang,[‡] Chi-Ming Che,[‡] and Tai-Chu Lau^{*†}

[†]Department of Biology and Chemistry and Institute of Molecular Functional Materials, City University of Hong Kong, Tat Chee Avenue, Hong Kong, China

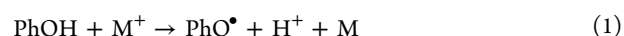
[‡]Department of Chemistry and State Key Laboratory of Synthetic Chemistry, The University of Hong Kong, Pokfulam Road, Hong Kong, China

S Supporting Information

ABSTRACT: Proton-coupled electron-transfer reactions of phenols have received considerable attention because of their fundamental interest and their relevance to many biological processes. Here we describe a remarkable four-electron oxidation of phenols by a (salen)ruthenium(VI) complex in the presence of pyridine in CH₃OH to afford (salen)ruthenium(II) *p*-benzoquinone imine complexes. Mechanistic studies indicate that this reaction occurs in two phases. The first phase is proposed to be a two-electron transfer process that involves electrophilic attack by Ru≡N at the phenol aromatic ring, followed by proton shift to generate a Ru(IV) *p*-hydroxyanilido intermediate. In the second phase the intermediate undergoes intramolecular two-electron transfer, followed by rapid deprotonation to give the Ru(II) *p*-benzoquinone imine product.

The reactivity of transition metal nitrido complexes (M≡N) has received much attention in recent years because these complexes are believed to be key intermediates in N₂ fixation; they are also useful reagents for the nitrogenation of organic substrates.¹ Group VIII nitrides are of particular interest because many of them exhibit novel electrophilic properties. For example, Meyer's group and others have shown that osmium(VI) nitrido complexes bearing polypyridyl or tris(pyrazolylborate) ligands are highly electrophilic and readily react with a variety of nucleophiles to form C–N, P–N, and E–N (E = O, S, Se) bonds.^{2–4} Novel electrophilic reactivity of iron nitrido complexes has also started to emerge.⁵ On the other hand, we have demonstrated that ruthenium(VI) nitrido complexes bearing salen ligands are highly electrophilic/oxidizing.^{6,7} For example, the complex [Ru^{VI}(N)(L)(CH₃OH)]⁺ (**1**, L = *N,N'*-bis-(salicylidene)-*o*-cyclohexyldiamine dianion) readily undergoes C–H activation of alkanes,⁸ aziridination of alkenes,⁹ nitrogeneration of alkynes,¹⁰ and C–N bond cleavage of anilines¹¹ under ambient conditions.

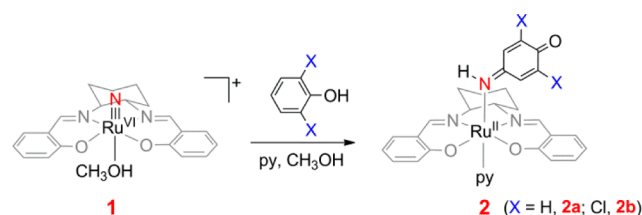
The oxidation of phenols, in particular their one-electron (1e) oxidation, has been extensively studied because of its relevance to many biological processes.^{12–19} Oxidation of phenols by 1e oxidants generally involves the formation of phenoxy radicals with coupled loss of the phenolic protons; i.e., it is a proton-coupled electron-transfer process that may involve stepwise or concerted pathways (eq 1).^{20–23} On the other hand, oxidation of



phenols by metal–oxo species may go through a H-atom abstraction mechanism (eq 2).^{24,25} A mechanism that involves initial electrophilic attack on the aromatic ring has also been proposed in the oxidation of phenol by [(bpy)₂(py)-Ru^{IV}(O)]²⁺.²⁶ However, there has been no report on the oxidation of phenol by a metal–nitrido species.

We report herein novel 4e oxidation of phenols to benzoquinone imines by **1** (Scheme 1). We provide direct

Scheme 1. Oxidation of Phenols to *p*-Benzoquinone Imines by **1**



evidence that these reactions are initiated by electrophilic attack of **1** at the aromatic rings of the phenols. **1** reacts rapidly with C₆H₅OH in CH₃OH at 25 °C to generate a species with λ_{max} = 616 nm (INT1), as monitored by UV–vis spectrophotometry (Figure S1). Analysis of the reaction mixture by electrospray ionization mass spectrometry (ESI-MS) shows a peak at *m/z* 562 that corresponds to the addition of C₆H₅OH (*M* = 94) to [Ru^{VI}(N)(L)(CH₃OH)]⁺ (*m/z* = 468) (Figure S2). Attempts to isolate this species were unsuccessful; apparently it is unstable and decomposes to [Ru^{III}(L)(CH₃OH)₂]⁺ during workup.

Reaction of **1** with C₆H₅OH was also carried out in the presence of 0.1 M pyridine (py), since it is known that py can enhance the reactivity of **1** through binding to the metal center *trans* to the nitrido ligand.^{8,9} The UV–vis spectral changes reveal the appearance of the same species (INT1) as in the absence of py (Figure 1a). However, in this case INT1 further reacts to give a product (**2a**) with λ_{max} = 665 nm (Figure 1b), and ESI-MS shows

Received: March 21, 2016

Published: April 25, 2016

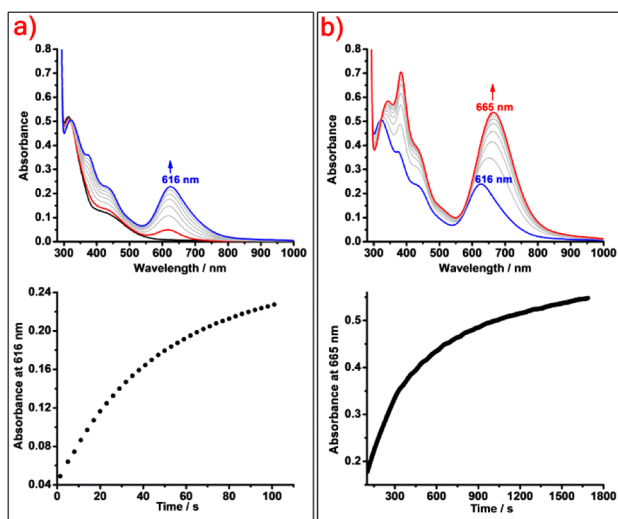


Figure 1. UV–vis spectral changes and the absorbance time trace for the reaction of **1** (5.00×10^{-5} M) with $\text{C}_6\text{H}_5\text{OH}$ (0.11 M) in 0.1 M py in CH_3OH at 25.0°C . (a) At 15 s intervals showing the first phase. (b) At 210 s intervals showing the second phase.

that this species has the composition $[\text{Ru}(\text{N})(\text{L})(\text{py})]^+ + \text{C}_6\text{H}_5\text{O}$ ($m/z = 608$, Figure S3). **2a** appears to be much more stable, and it could be isolated and shown to be the Ru(II) *p*-benzoquinone imine complex $[\text{Ru}^{\text{II}}(\text{L})(\text{HN-}p\text{-C}_6\text{H}_4\text{O})(\text{py})]$. Similarly, reaction of **1** with 2,6-dichlorophenol in the presence of py afforded $[\text{Ru}^{\text{II}}(\text{L})(\text{HN-}2,6\text{-Cl}_2\text{-}p\text{-C}_6\text{H}_3\text{O})(\text{py})]$ (**2b**).

The structures of **2a** (Figure S4) and **2b** (Figure 2) have been determined by X-ray crystallography. The crystal data and

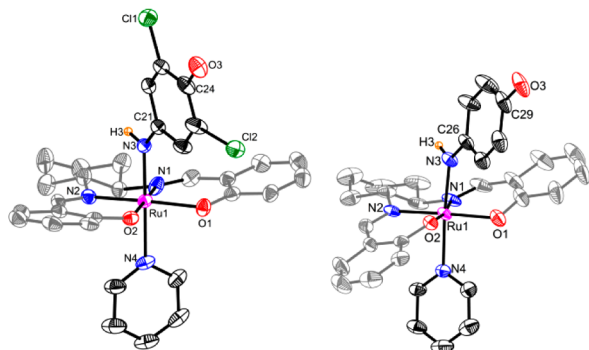


Figure 2. Molecular structures of **2b** (left) and the cation of **3** (right). Thermal ellipsoids are drawn at 50% probability. H-atoms (except H3) and solvent molecules have been omitted for clarity. Selected bond lengths (Å) and angles (deg): Ru(1)–N(3) 1.936(2) (**2b**), 2.031(5) (**3**); Ru(1)–N(4) 2.154(2) (**2b**), 2.125(5) (**3**); N(3)–C(21)/C(26) 1.344(3) (**2b**), 1.301(8) (**3**); C(24)/C(29)–O(3) 1.253(3) (**2b**), 1.239(8) (**3**); Ru(1)–N(3)–C(21)/C(26) 131.8(2) (**2b**), 130.9(5) (**3**).

structure refinement details for **2b** are given in Table S1, but the data for **2a** are not good enough for bond data discussion. A similar Ru(II) *p*-benzoquinone imine complex $[\text{Ru}^{\text{II}}(\text{NH}_3)_5(\text{HN-}p\text{-C}_6\text{H}_4\text{O})]^{2+}$ has been synthesized by the reaction of $[\text{Ru}^{\text{II}}(\text{NH}_3)_5\text{Cl}]^{2+}$ with *p*-aminophenol, but no X-ray structure was reported.²⁷ Both **2a** and **2b** have a distorted octahedral geometry, with the salen ligand coordinated to the Ru center in the equatorial plane and an axial py ligand. The other axial site is occupied by a *p*-benzoquinone imine ligand in **2a** and 2,6-dichloro-*p*-benzoquinone imine in **2b**. In the benzoquinone

imine ligand of **2b**, the bond distances of N(3)–C(21) [1.344(3) Å] and C(24)–O(3) [1.253(3) Å] are consistent with C=N and C=O bonds, respectively. The rather short Ru(1)–N(3) (Ru–N_{imine}) bond distance of 1.936(2) Å, compared to 2.154(2) Å for Ru(1)–N(4) (Ru–N_{py}), is indicative of strong π -back-bonding between Ru^{II} and the benzoquinone imine ligand.

Complexes **2a** and **2b** have also been characterized by various spectroscopic techniques. The ¹H NMR spectra (Figures S5 and S6) of the complexes exhibit well-resolved signals at normal fields, consistent with their formulation as diamagnetic d⁶ Ru(II) complexes. The N–H resonances of **2a** and **2b** occur as singlets at 13.21 and 13.35 ppm, respectively; these resonances disappear upon D₂O addition. The N–H resonance for free *p*-benzoquinone imine occurs at 12.07 ppm (recorded in ether).²⁸ ESI-MS of **2a** and **2b** show the parent M⁺ peak at m/z 608 and 676, respectively (Figure S7); the neutral **2a** and **2b** are most likely oxidized to 1+ ions during the ESI process. In the IR spectra the $\nu(\text{N-H})$ stretch of **2a** and **2b** occurs at 3173 and 3167 cm⁻¹, respectively (Figure S8). The UV–vis spectra of **2a** and **2b** (Figure S9) exhibit an intense band at 665 and 672 nm ($\epsilon_{\text{max}} = 20\,000$ and $22\,300$ mol⁻¹ dm³ cm⁻¹), respectively, which is attributed to Ru(II) to benzoquinone imine charge-transfer transition. The cyclic voltammogram (CV) of **2a** exhibits two reversible waves at $E_{1/2} = +0.72$ and -0.25 V (versus Cp₂Fe⁺⁰), where Cp = $\eta^5\text{-C}_5\text{H}_5$, which are assigned to the Ru^{IV/III} and Ru^{III/II} couples, respectively (Figure 3). For $[\text{Ru}^{\text{III}}(\text{L})(\text{py})_2]^+$, the

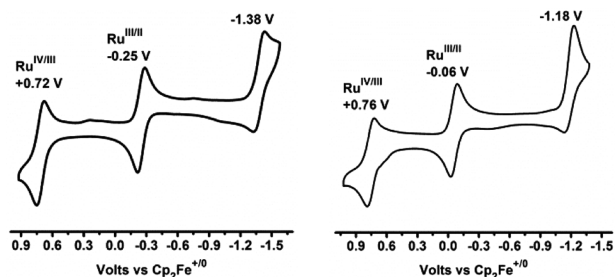


Figure 3. CVs of **2a** (left) and **2b** (right) in CH_3CN .

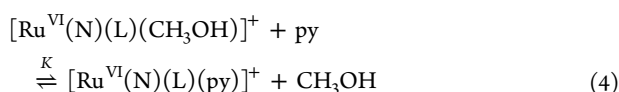
Ru^{IV/III} and Ru^{III/II} couples occur at $E_{1/2} = +0.69$ and -0.58 V, respectively (Table S2).²⁹ The large anodic shift of the Ru^{III/II} couple (330 mV) in **2a** relative to $[\text{Ru}^{\text{III}}(\text{L})(\text{py})_2]^+$ again indicates that benzoquinone imine is a much better π -acceptor ligand than py, in line with the relatively short Ru–N_{imine} bond. In **2b** the Ru^{IV/III} and Ru^{III/II} waves appear at $E_{1/2} = +0.76$ and -0.06 V, respectively, indicating that the π -accepting ability of benzoquinone imine ligand is further enhanced by the electron-withdrawing chloro substituents. There is also a quasi-reversible wave at $E_{1/2} = -1.38$ and -1.18 V for **2a** and **2b**, respectively, which is tentatively assigned to the 1e reduction of the benzoquinone imine ligand.

In accordance with the electrochemical data, **2a** is readily oxidized by $[\text{Cp}_2\text{Fe}](\text{PF}_6)$ in CH_3OH to generate the dark purple compound $[\text{Ru}^{\text{III}}(\text{L})(\text{HN-}p\text{-C}_6\text{H}_4\text{O})(\text{py})](\text{PF}_6)$ (**3**) in 70% yield. The molecular structure of **3** has also been determined by X-ray crystallography (Figure 2). Notably, the Ru–N_{imine} bond [Ru(1)–N(3) = 2.031(5) Å] in **3** is longer than that in **2b** by ca. 0.1 Å (1.936(2) Å), despite Ru having a higher oxidation state, which is consistent with strong π -back-bonding between Ru^{II} and benzoquinone imine. As expected for a d⁵ Ru^{III} compound, **3** has a room-temperature magnetic moment of $\mu_{\text{eff}} = 1.93 \mu_{\text{B}}$ (Guoy method). ESI-MS shows the parent M⁺ peak at $m/z = 608$. In the IR spectrum the $\nu(\text{N-H})$ stretch occurs at

3268 cm^{-1} , and a strong $\nu(\text{P-F})$ band is found at 845 cm^{-1} (Figure S8).

Kinetic studies on the reaction of **1** with phenol in CH_3OH in the presence of py have been carried out by UV-vis spectrophotometry. The UV-vis spectral changes in CH_3OH at 25.0 °C indicate that this reaction consists of two phases (Figure 1). The final spectrum is the same as that of **2a** with a peak at $\lambda_{\text{max}} = 665 \text{ nm}$ (Figure S9). This indicates that the reaction is highly selective and only the *para* product is formed. Ortho attack is unfavorable, presumably due to steric effects. In the presence of excess PhOH and py, pseudo-first-order kinetics were observed for the first phase, and the pseudo-first-order rate constant, k_{obs} , was found to increase linearly with $[\text{PhOH}]$ and $[\text{py}]$ (Figure 4) according to the rate law shown in eq 3:

$$-\text{d}[\text{Ru}^{\text{VI}}\text{N}]/\text{d}t = k_{\text{obs}}[\text{RuN}] \\ = \{k_a + Kk_b[\text{py}]\}[\text{Ru}^{\text{VI}}\text{N}][\text{PhOH}] \quad (3)$$



$$\text{d}[\text{Ru}^{\text{II}}]/\text{d}t = K'k_c[\text{Ru}^{\text{VI}}\text{N}][\text{PhOH}] \quad (5)$$

K is the equilibrium constant for the binding of py with **1** (eq 4) (see discussion below). At 25.0 °C, k_a and Kk_b are found to be $(1.24 \pm 0.11) \times 10^{-1} \text{ M}^{-1} \text{ s}^{-1}$ and $(1.02 \pm 0.06) \text{ M}^{-2} \text{ s}^{-1}$, respectively. No kinetic isotope effect (KIE) was found when $\text{C}_6\text{H}_5\text{OD}$ in CD_3OD ($\text{KIE} = 0.92 \pm 0.06$) or $\text{C}_6\text{D}_5\text{OH}$ in CH_3OH ($\text{KIE} = 1.03 \pm 0.05$) was used as substrate (Table S3, Figure S10), suggesting that no O-H or C-H bond cleavage occurs in the rate-determining step.

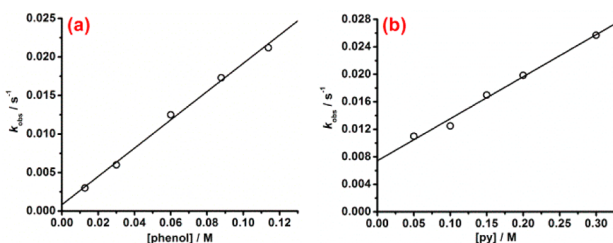


Figure 4. (a) Plot of k_{obs} vs $[\text{phenol}]$ for the first phase of the reaction of **1** with phenol in 0.1 M py in CH_3OH at 25.0 °C. Slope = $(1.84 \pm 0.07) \times 10^{-1}$; y -intercept = $(8.32 \pm 4.89) \times 10^{-4}$; $r^2 = 0.99$. (b) Plot of k_{obs} vs $[\text{py}]$ for the first phase of the reaction of **1** with phenol (0.06 M) in CH_3OH at 25.0 °C. Slope = $(6.11 \pm 0.37) \times 10^{-2}$; y -intercept = $(7.43 \pm 0.68) \times 10^{-3}$; $r^2 = 0.99$.

The rate of the second phase is independent of $[\text{phenol}]$ (0.01–0.12 M) but depends linearly on $[\text{py}]$ (Figure 5),³⁰ with the rate law shown in eq 5. K' is the equilibrium constant for the binding of the Ru(IV) intermediate with py (see discussion below). At 25.0 °C, $K'k_c$ was found to be $(9.32 \pm 0.41) \times 10^{-3} \text{ M}^{-1} \text{ s}^{-1}$. No KIE was found when $\text{C}_6\text{H}_5\text{OD}$ in CD_3OD ($\text{KIE} = 0.97 \pm 0.08$) was used as substrate (Figure S11). When $\text{C}_6\text{D}_5\text{OH}$ in CH_3OH was used, $\text{KIE} = 1.32 \pm 0.07$ was observed (Figure S11), which is probably a secondary KIE (Table S3).

Similar kinetic behavior was observed for the reaction of **1** with various 2,6-disubstituted phenols (2,6- $\text{X}_2\text{-C}_6\text{H}_3\text{OH}$) in the presence of py. The second-order rate constants (at $[\text{py}] = 0.1 \text{ M}$) for the first phase follow the order of X (relative rate) = MeO (208) > $t\text{Bu}$ (61) > Me (27) > H (5) > Br (2) > Cl (1) (Table S4). The increase in rate with electron-donating substituents is

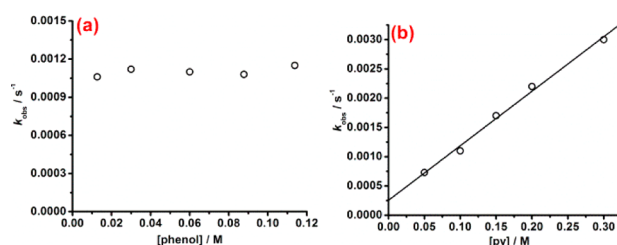
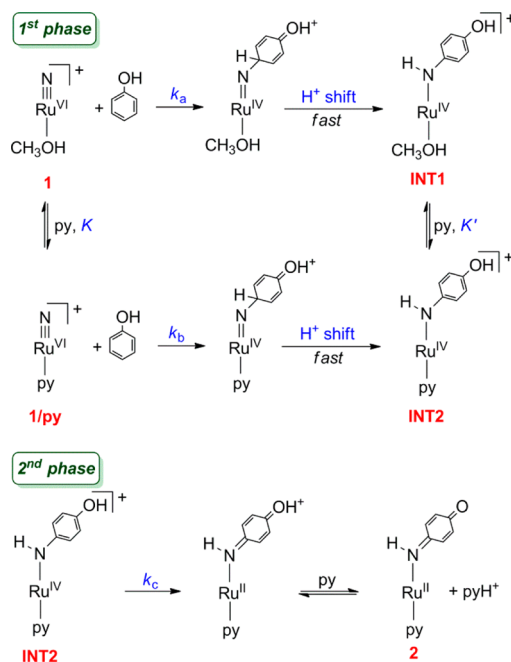


Figure 5. (a) Plot of k_{obs} vs $[\text{phenol}]$ for the second phase of the reaction of **1** with phenol in 0.1 M py in CH_3OH at 25.0 °C. (b) Plot of k_{obs} vs $[\text{py}]$ for the second phase of the reaction of **1** with phenol (0.06 M) in CH_3OH at 25.0 °C. Slope = $(9.32 \pm 0.41) \times 10^{-3}$; y -intercept = $(2.55 \pm 0.75) \times 10^{-4}$; $r^2 = 0.99$.

consistent with a mechanism that involves electrophilic attack by **1** at the phenols. Product analysis by ESI-MS revealed the formation of the corresponding ruthenium benzoquinone imine complexes (Figure S12). On the other hand, when **1** was treated with a *para*-substituted phenol such as *p*-MeO- $\text{C}_6\text{H}_4\text{OH}$ in the presence of py, the spectral changes were similar to those in the absence of the phenol (Figure S13), and product analysis by ESI-MS revealed the formation of $[\text{Ru}^{\text{III}}(\text{L})(\text{py})(\text{CH}_3\text{OH})]^+$ (Figure S14). This indicates that the predominant reaction in this case is N...N coupling,²⁹ and direct reaction of **1** with *p*-MeO- $\text{C}_6\text{H}_4\text{OH}$ is much slower.

Based on the experimental results, a proposed mechanism for the reaction of **1** with phenol in the presence of py is shown in Scheme 2. The first phase involves initial equilibrium binding of **1**

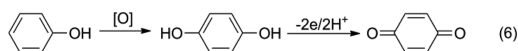
Scheme 2. Proposed Mechanism for the 4e Oxidation of Phenol by **1** in the Presence of py (the Salen Ligand Is Omitted for Clarity)



with py to give $[\text{Ru}^{\text{VI}}(\text{N})(\text{L})(\text{py})]^+$ (**1/py**). This is followed by parallel electrophilic attack by **1** and **1/py** at the *para* position of the aromatic ring to generate the Ru(IV) *p*-hydroxyanilido species (intermediates INT1 and INT2); this step is analogous to attack on aromatic rings of phenols by electrophiles such as Br^+ or NO_2^+ .³¹ This proposed mechanism is consistent with the

observed rate law (eq 3) under the conditions that $K[\text{py}] \ll 1$. Although $K = 15.6 \pm 1.1 \text{ M}^{-1}$ in $\text{ClCH}_2\text{CH}_2\text{Cl}$,⁹ it is expected to be much smaller in a coordinating solvent such as CH_3OH . This is supported by the observation of little or no change in the UV–vis spectrum upon addition of py (0.1 M) to **1** ($5 \times 10^{-5} \text{ M}$) in CH_3OH (Figure S15). The spectral changes for the reaction of **1** with PhOH in CH_3OH are also very similar to those in the presence of py. The lack of KIE when $\text{C}_6\text{H}_5\text{OD}$ or $\text{C}_6\text{D}_5\text{OH}$ was used as substrate is in line with the electrophilic ring attack mechanism. In the second phase the Ru(IV) intermediate INT2 undergoes intramolecular 2e transfer followed by rapid deprotonation to give the Ru(II) *p*-benzoquinone imine product. Since in the absence of py no Ru(II) benzoquinone imine could be observed or isolated, this suggests that INT2, although present as a minor species, is the reactive intermediate, while INT1 is relatively unreactive. Since py is a π -acid ligand that is known to stabilize Ru^{II} , which is a good π -base, its binding to Ru^{IV} is expected to facilitate the intramolecular redox reaction. Hence, INT2 should be much more reactive than INT1. Again $K'[\text{py}] \ll 1$ is expected; thus, the rate law for this step is as shown in eq 5.

In summary, we have reported remarkable 4e oxidation of phenols by a Ru(VI) nitrido complex. This reaction occurs by two consecutive 2e phases. The first phase involves electrophilic attack of **1** at the aromatic ring to generate the Ru(IV) *p*-hydroxyanilido intermediate. In the second phase py-assisted intramolecular redox reaction occurs to give the Ru(II) *p*-benzoquinone imine product. This reaction is analogous to the 4e oxidation of phenol by a metal–oxo species, in which the phenol is first oxidized to hydroquinone and then to benzoquinone (eq 6).²⁶



■ ASSOCIATED CONTENT

Supporting Information

The Supporting Information is available free of charge on the ACS Publications website at DOI: 10.1021/jacs.6b02923.

- Experimental details and characterization data (PDF)
- X-ray crystallographic data for **2b** (CIF)
- X-ray crystallographic data for **3** (CIF)

■ AUTHOR INFORMATION

Corresponding Author

*bhtclau@cityu.edu.hk

Notes

The authors declare no competing financial interest.

■ ACKNOWLEDGMENTS

The work described in this paper was supported by the Hong Kong University Grants Committee Areas of Excellence Scheme (AoE/P-03/08) and the Research Grants Council of Hong Kong (CityU 101612).

■ REFERENCES

- (1) (a) Du Bois, J.; Tomooka, C. S.; Hong, J.; Carreira, E. M. *Acc. Chem. Res.* **1997**, *30*, 364. (b) Eikey, R. A.; Abu-Omar, M. M. *Coord. Chem. Rev.* **2003**, *243*, 83. (c) Berry, J. F. *Comments Inorg. Chem.* **2009**, *30*, 28. (d) Hohenberger, J.; Ray, K.; Meyer, K. *Nat. Commun.* **2012**, *3*, 720. (e) Smith, J. M. *Prog. Inorg. Chem.* **2014**, *58*, 417.
- (2) Selected examples: (a) Huynh, M. H. V.; El-Samanody, E.-S.; Demadis, K. D.; Meyer, T. J.; White, P. S. *J. Am. Chem. Soc.* **1999**, *121*,

1403. (b) Huynh, M. H. V.; White, P. S.; Meyer, T. J. *J. Am. Chem. Soc.* **2001**, *123*, 9170. (c) Huynh, M. H. V.; White, P. S.; Carter, C. A.; Meyer, T. J. *Angew. Chem., Int. Ed.* **2001**, *40*, 3037. (d) Huynh, M. H. V.; Morris, D. E.; White, P. S.; Meyer, T. J. *Angew. Chem., Int. Ed.* **2002**, *41*, 2330. (e) Huynh, M. H. V.; Baker, R. T.; Jameson, D. L.; Labouriau, A.; Meyer, T. J. *J. Am. Chem. Soc.* **2002**, *124*, 4580. (f) Meyer, T. J.; Huynh, M. H. V. *Inorg. Chem.* **2003**, *42*, 8140.

- (3) Selected examples: (a) Crevier, T. J.; Mayer, J. M. *J. Am. Chem. Soc.* **1998**, *120*, 5595. (b) Crevier, T. J.; Lovell, S.; Mayer, J. M.; Rheingold, A. L.; Guzei, I. A. *J. Am. Chem. Soc.* **1998**, *120*, 6607. (c) McCarthy, M. R.; Crevier, T. J.; Bennett, B.; Dehestani, A.; Mayer, J. M. *J. Am. Chem. Soc.* **2000**, *122*, 12391. (d) Dehestani, A.; Kaminsky, W.; Mayer, J. M. *Inorg. Chem.* **2003**, *42*, 605.

- (4) (a) Brown, S. N. *J. Am. Chem. Soc.* **1999**, *121*, 9752. (b) Brown, S. N. *Inorg. Chem.* **2000**, *39*, 378. (c) Maestri, A. G.; Cherry, K. S.; Toboni, J. J.; Brown, S. N. *J. Am. Chem. Soc.* **2001**, *123*, 7459.

- (5) Selected examples: (a) Scepaniak, J. J.; Young, J. A.; Bontchev, R. P.; Smith, J. M. *Angew. Chem., Int. Ed.* **2009**, *48*, 3158. (b) Scepaniak, J. J.; Vogel, C. S.; Khusniyarov, M. M.; Heinemann, F. W.; Meyer, K.; Smith, J. M. *Science* **2011**, *331*, 1049. (c) Scepaniak, J. J.; Bontchev, R. P.; Johnson, D. L.; Smith, J. M. *Angew. Chem., Int. Ed.* **2011**, *50*, 6630. (d) Lee, W. T.; Juarez, R. A.; Scepaniak, J. J.; Muñoz, S. B., III; Dickie, D. A.; Wang, H.; Smith, J. M. *Inorg. Chem.* **2014**, *53*, 8425. (e) Muñoz, S. B., III; Lee, W. T.; Dickie, D. A.; Scepaniak, J. J.; Subedi, D.; Pink, M.; Johnson, M. D.; Smith, J. M. *Angew. Chem., Int. Ed.* **2015**, *54*, 10600.

- (6) Man, W. L.; Tang, T. M.; Wong, T. W.; Lau, T. C.; Peng, S. M.; Wong, W. T. *J. Am. Chem. Soc.* **2004**, *126*, 478.

- (7) Man, W. L.; Lam, W. W. Y.; Lau, T. C. *Acc. Chem. Res.* **2014**, *47*, 427.

- (8) Man, W. L.; Lam, W. W. Y.; Kwong, H. K.; Yiu, S. M.; Lau, T. C. *Angew. Chem., Int. Ed.* **2012**, *51*, 9101.

- (9) Man, W. L.; Lam, W. W. Y.; Yiu, S. M.; Lau, T. C.; Peng, S. M. *J. Am. Chem. Soc.* **2004**, *126*, 15336.

- (10) Man, W. L.; Xie, J.; Lo, P. K.; Lam, W. W. Y.; Yiu, S. M.; Lau, K. C.; Lau, T. C. *Angew. Chem., Int. Ed.* **2014**, *53*, 8463.

- (11) Man, W. L.; Xie, J.; Pan, Y.; Lam, W. W. Y.; Kwong, H. K.; Ip, K. W.; Yiu, S. M.; Lau, K. C.; Lau, T. C. *J. Am. Chem. Soc.* **2013**, *135*, 5533.

- (12) Halliwell, B.; Gutteridge, J. M. C. *Free Radicals in Biology and Medicine*, 2nd ed.; Oxford University Press: Oxford, Great Britain, 1989.

- (13) Burton, G. W.; Ingold, K. U. *Acc. Chem. Res.* **1986**, *19*, 194.

- (14) Tommos, C.; Babcock, G. T. *Biochim. Biophys. Acta, Bioenerg.* **2000**, *1458*, 199.

- (15) Renger, G. *Biochim. Biophys. Acta, Bioenerg.* **2004**, *1655*, 195.

- (16) Meyer, T. J.; Huynh, M. H. V.; Thorp, H. H. *Angew. Chem., Int. Ed.* **2007**, *46*, 5284.

- (17) Stubbe, J.; Nocera, D. G.; Yee, C. S.; Chang, M. C. Y. *Chem. Rev.* **2003**, *103*, 2167.

- (18) Webster, R. D. *Acc. Chem. Res.* **2007**, *40*, 251.

- (19) Huynh, M. H. V.; Meyer, T. J. *Chem. Rev.* **2007**, *107*, 5004.

- (20) Markle, T. F.; Rhile, I. J.; DiPasquale, A. G.; Mayer, J. M. *Proc. Natl. Acad. Sci. U. S. A.* **2008**, *105*, 8185.

- (21) Song, N.; Stanbury, D. M. *Inorg. Chem.* **2008**, *47*, 11458.

- (22) Song, N.; Stanbury, D. M. *Inorg. Chem.* **2012**, *51*, 4909.

- (23) Bonin, J.; Costentin, C.; Louault, C.; Robert, M.; Routier, M.; Savéant, J. *Proc. Natl. Acad. Sci. U. S. A.* **2010**, *107*, 3367.

- (24) Al-Ajlouni, A.; Bakac, A.; Espenson, J. H. *Inorg. Chem.* **1993**, *32*, 5792.

- (25) Yiu, D. T. Y.; Lee, M. F. W.; Lam, W. W. Y.; Lau, T. C. *Inorg. Chem.* **2003**, *42*, 1225.

- (26) Seok, W. K.; Meyer, T. J. *J. Am. Chem. Soc.* **1988**, *110*, 7358.

- (27) Rieder, K.; Hauser, U.; Siegenthaler, H.; Schmidt, E.; Ludi, A. *Inorg. Chem.* **1975**, *14*, 1902.

- (28) Lerner, L. J. *Phys. Chem. A* **2011**, *115*, 9901.

- (29) Man, W. L.; Kwong, H. K.; Lam, W. W. Y.; Xiang, J.; Wong, T. W.; Lam, W. H.; Wong, W. T.; Peng, S. M.; Lau, T. C. *Inorg. Chem.* **2008**, *47*, 5936.

- (30) The small intercept in Figure Sb could be due to a slow decomposition of INT1.

- (31) Smith, M. B.; Marsh, J. *March's Advanced Organic Chemistry*, 5th ed., Wiley: New York, 2001; p 675.